Title: Entorhinal tau predicts hippocampal activation and memory deficits in Alzheimer's disease

Running Title: Tau and hippocampal activation in Alzheimer's

Nils Richter, MD [1,2*], Gérard Bischof, PhD [2,3], Julian Dronse, MD [1,2], Nils Nellessen, MD [12], Bernd Neumaier, PhD [4,5], Karl-Josef Langen, MD[6], Alexander Drzezga, MD [3], Gereon R. Fink, MD [1,2], Thilo van Eimeren, MD [1,3], Juraj Kukolja, MD [1,2,7], Oezguer A. Onur, MD [1,2]

[1] Department of Neurology, Faculty of Medicine and University Hospital Cologne, University of Cologne, 50937 Cologne, Germany

[2] Cognitive Neuroscience, Institute of Neuroscience and Medicine (INM-3), Research Center Jülich, 52425 Jülich, Germany

[3] Department of Nuclear Medicine, Faculty of Medicine and University Hospital Cologne, University of Cologne, 50937 Cologne, Germany

[4] Nuclear Chemistry, Institute of Neuroscience and Medicine (INM-5), Research Center Jülich, 52425 Jülich, Germany

[5] Institute for Radiochemistry and Experimental Molecular Imaging, Faculty of Medicine and University Hospital Cologne, University of Cologne, 50937 Cologne, Germany

[6] Medical Imaging Physics, Institute of Neuroscience and Medicine (INM-4), Research Center Jülich, 52425 Jülich, Germany

[7] Department of Neurology and Neurophysiology, Helios University Hospital Wuppertal, 42283 Wuppertal, Germany

**Corresponding author:*
Nils Richter
Cognitive Neuroscience
Institute for Neuroscience and Medicine, INM-3
Research Center Jülich
52425 Jülich
Germany
Phone: +49-(0)2461-61-9173
Fax: +49-(0)2461-61-1518
E-mail: n.richter@fz-juelich.de

Abstract (247/250 words)

Background: To date, it remains unclear how amyloid plaques and neurofibrillary tangles are related to neural activation and, consequently, cognition in Alzheimer's disease (AD). Recent findings indicate that tau accumulation may drive hippocampal hyperactivity in cognitively normal aging, but it remains to be elucidated how tau accumulation is related to neural activation in AD.

Objective: To determine whether the association between tau accumulation and hippocampal hyperactivation persists in MCI and mild dementia or if the two measures dissociate with disease progression, we investigated the relationship between local tau deposits and memory-related neural activation in MCI and mild dementia due to AD.

Methods: Fifteen patients with MCI or mild dementia due to AD underwent a neuropsychological assessment and performed an item memory task during functional magnetic resonance imaging. Cerebral tau accumulation was assessed using positron emission tomography and [^{18}F]-AV-1451.

Results: Entorhinal, but not global tau accumulation, was highly correlated with hippocampal activation due to visual item memory encoding and predicted memory loss over time. Neural activation in the posterior cingulate cortex and the fusiform gyrus was not significantly correlated with tau accumulation.

Conclusion: These findings extend previous observations in cognitively normal aging, demonstrating that entorhinal tau continues to be closely associated with hippocampal hyperactivity and memory performance in MCI and mild dementia due to AD. Furthermore, data suggest that this association is strongest in medial temporal lobe structures. In summary, our data provide novel insights into the relationship of tau accumulation to neural activation and memory in AD.

Keywords: AV-1451, fMRI, MCI, dementia, positron emission tomography

Introduction

Alzheimer's disease typically presents with progressive loss of episodic memory and is histopathologically characterized by amyloid plaques and neurofibrillary tangles. Amyloid deposition is assumed to precede the accumulation of pathological tau protein, followed by neuronal injury, and eventually, the mnestic and cognitive decline [1,2]. In this context, the interaction between neuronal activation, pathological protein aggregates, and mnestic and cognitive functions remains elusive.

Individuals at risk of developing Alzheimer's disease, because of genetic mutations associated with familial Alzheimer's disease [3,4] or apolipoprotein E4 positivity [5,6] have consistently been demonstrated to exhibit increased neural activation in the hippocampus compared to non-carriers. While this observation suggests that amyloid-ß accumulation may play a role in hippocampal hyperactivation in cognitively healthy individuals, findings regarding the association between amyloid-ß and hippocampal functional MRI (fMRI) activation in cognitively healthy older adults have been ambiguous [7–11]. Recent multimodal imaging studies measuring amyloid and tau accumulation, as well as hippocampal activation, in cognitively healthy seniors [10,12,13] provide a possible explanation: hippocampal hyperactivation may be more closely related to the tau accumulation that follows amyloid build-up, than to the amyloid deposition [12].

At the stage of mild cognitive impairment (MCI), findings regarding changes in the hippocampus's neural activation are less consistent than in cognitively normal individuals. Using functional magnetic resonance imaging (fMRI), several studies reported increased hippocampal activation during memory tasks compared to cognitively healthy controls [14–18] while others did not [19–21]. This discrepancy has been attributed to different disease stages [22] and the amyloid status [23].

Furthermore, it remains to be investigated which role tau accumulation plays concerning memory relevant neuronal activation in Alzheimer's disease as cognitive deficits become apparent. Changes in neural activation could reflect compensation [9,15] or disease propagation [24,25]. Given conflicting findings regarding memory-related neural activation in MCI, it is conceivable that tau accumulation continues to be positively correlated with neuronal activation in the presence of cognitive deficits. However, it is also possible that this relationship disappears as an increasing number of neurons is lost.

Using fMRI of a visual item memory task and non-invasive *in-vivo* imaging of tau accumulation with [^{18}F]-AV1451-PET, we, therefore, investigated in a group of Alzheimer's disease patients, whether the positive correlation between tau accumulation and hippocampal hyperactivation previously described in cognitively healthy older adults persists in the presence of mnestic and cognitive deficits. Generally, this visual memory task detects the subsequent memory effect (SME) on neural activation, i.e., greater activation for subsequently remembered stimuli than for forgotten stimuli in the hippocampus and the fusiform gyrus and deactivation of posterior midline structures [26]. Using this task, we have previously compared patients with MCI and CSF-biomarkers indicative of AD to age-matched controls: MCI was associated with a smaller SME on activation in the hippocampus and fusiform gyrus and less task-related deactivation in the posterior cingulate cortex (PCC) [27]. However, to date, it is unknown how changes in task-related neural activation are related to local or global tau accumulation.

We hypothesized that entorhinal tau accumulation in Alzheimer's disease patients is correlated with episodic memory function and that this tau accumulation is correlated with visual item memory task-induced neural activation. To determine whether the association between tau accumulation and neuronal activation is specific to the medial

temporal lobe structures, we also investigated this relationship in the fusiform gyrus, which typically activates during encoding of visual content, and the posterior cingulate cortex, which typically deactivates during encoding of visual content [26–29].

Methods

Participants

Twenty patients recently diagnosed with MCI or mild dementia due to Alzheimer's disease (13 male, 7 female, 55 – 82 years old), who had undergone an AV-1451-PET during clinical work-up, were recruited. Five patients had to be excluded from further analyses because they were unable to perform the functional task (two) or due to excessive head motion during fMRI (three). Thus, the data of 15 patients entered further analyses (**Table 1**).

The main inclusion criteria were positive biomarkers indicative of Alzheimer's pathology and signs of neuronal injury, meeting the criteria for a high likelihood of Alzheimer's disease [30,31]. Evidence of neuronal injury was operationalized as i) medial temporal atrophy according to the medial temporal atrophy scale [32] on T1-weighted images, ii) temporoparietal and precuneal hypometabolism in fluorodeoxyglucose-PET quantified with 3D-SSP [33], or iii) elevated total Tau-protein in CSF (> 375pg/ml). Positive amyloid pathology was defined as CSF Amyloid $ß_{1-42}$ < 550pg/ml, a Tau/Amyloid-$ß_{1-42}$ ratio > 0.52 [34], or a positive amyloid PET during clinical work-up. Importantly, all patients also exhibited strong AV-1451 binding in temporoparietal regions. Exclusion criteria were neurological conditions besides AD, major psychiatric disease, other medical conditions that could affect cognition, inability to give informed consent, MRI exclusion criteria such as claustrophobia, cardiac pacemakers, and other non-MR-compatible implants.

Furthermore, patients were excluded if structural lesions were detected on cerebral imaging.

All participants underwent a neurological examination by a neurologist and a comprehensive neuropsychological assessment, as previously described [27]. All patients predominantly had memory impairments, but the majority also had some executive deficits and lesser language impairments.

Independence in activities of daily living was assessed using the history given by caregivers and with the Bayer Activities of Daily Living Scale (cut-off < 5). Based on these measures, four patients were demented. The four patients with dementia did not differ significantly from the MCI patients with respect to age ($t_{(13)}$ = .112, 95%-CI [-8.714, 9.669]), education ($t_{(13)}$ = 1.122, 95%-CI [-2.123, 6.713]), performance on the MMST ($t_{(13)}$ = .553, 95%-CI [-2.838, 4.793]), or gender ($x^2_{(1)}$ = .170, p = .680).

Disease severity of the demented patients was defined based on the history given by caregivers and the MMSE [35,36].

Twelve patients took cholinesterase inhibitors; three patients also took antidepressant medication. All doses of medication had been stable during the weeks before fMRI scanning. The average delay between the Tau-PET and the fMRI was 207.47 days (standard deviation 191.71 days).

The ethics committee of the medical faculty of the University of Cologne approved the study. Written informed consent was obtained from all participants before the study following the Declaration of Helsinki.

Procedure

Clinical, neuropsychological, and MRI data were obtained within a month. During fMRI scanning, participants performed a visual item memory task consisting of an encoding (duration: 10 minutes) and a retrieval phase (duration: 17 minutes) spaced

seven minutes apart. During encoding, a fixation cross was presented at the center of the screen, where 80 photographs of natural or artificial items were presented. Items were shown for 3.5s each, with an inter-trial-interval of 1s, in random order. Forty null-events, showing only the fixation cross, were randomly interspersed, resulting in variable stimulus-onset asynchronies. Participants were asked to memorize each object and indicate via button press with the index or middle finger of the right hand, whether the object was "natural" such as an animal, fruit, or vegetable, or "artificial", i.e., human-made or modified. During the retrieval period, a fixation cross was again present at the center of the screen. Eighty stimuli were presented during encoding, and 40 new objects were shown in random order for 3.5s each, with an inter-trial-interval of 2s. Stimuli were displayed using the software Presentation (Neurobehavioural systems, Albany, CA, USA) via a screen situated behind the scanner. Participants viewed the screen via a mirror mounted on the head coil. Participants were instructed to indicate via button press with the middle or index finger of their right hand, whether the object was "old", i.e., had been presented during encoding, or "new", i.e., had not been presented previously. During the retrieval period, 60 null-events were interspersed randomly. The task was rehearsed outside and inside the MR scanner before scanning. For this rehearsal, a shortened version of the paradigm and a separate set of stimuli were used.

Behavioral data analysis

Trials with reaction times less than 400ms or more than two standard deviations greater than the mean were considered outliers and classified as invalid trials together with missed trials. The analysis focused on items that were correctly classified during the retrieval session. The performance was assessed using the sensitivity index *d'*, the difference between hit rate (*H*; previously seen items classified as "old" divided by all

previously seen items) and false-alarm rate (*F*; new items classified as "old" divided by all new items) in standard deviation units [37]: $d' = \Phi^{-1}(H') - \Phi^{-1}(F')$. Since the performance in this task is not solely dependent on hippocampal memory formation but also stimulus processing [26], we additionally derived two modality-independent measures of memory performance from the neuropsychological assessment: (i) Performance on the delayed recall of memory tests as a parameter most sensitive to deficits in episodic memory [38] and, (ii) the number of items forgotten during the delay period (information initially reproduced minus information reproduced in the delayed recall) as an estimate for memory consolidation and resilience to interference [38–40]. Composite delayed recall and memory loss scores were computed from visual and verbal memory scores to generate measures independent of the type of content. Specifically, raw test scores from the VLMT (the German version of the Rey Auditory Learning Test [38]), and the Rey-Osterrieth Complex Figure Test [41] were z-transformed and averaged.

Neuropsychological, demographic, and ROI measures were normally distributed as assessed with Shapiro-Wilks tests. The delay between PET and MRI measurements, as well as medication, were not normally distributed. All statistical analyses not performed at the voxel level were conducted with SPSS (Version 24.0, IBM Corp., Armonk, NY). In the present sample, none of the neuropsychological measures or values from ROIs that entered statistical analyses, except for the cortical thickness of the entorhinal cortex, were correlated with age. To account for the large number of correlations that were computed, correction for multiple comparisons was performed by controlling the false discovery rate (FDR) [42]. Correlations significant after FDR-correction ($p < 0.0068$) for multiple comparisons are highlighted in the results section. Significant correlations of tau accumulation with fMRI or cognitive measures were also computed as partial correlations, correcting for the delay between MRI and PET

measurements and psychoactive medication. Likewise, significant correlations between cognitive and fMRI measures were computed as partial correlations, corrected for psychoactive medication. Statistical values for correlations that were not significant can be found in **Supplementary Table 1**.

All statistical tests were performed using robust methods with bootstrapping to account for the small sample size and non-normal distribution of a subset of variables. Results are, therefore, presented with 95% confidence intervals (CI).

MR and PET acquisition

The PET scans were collected using a PET-CT Siemens Biograph mCT Flow 128 Edge (Siemens). A low-dose transmission scan was performed for attenuation correction before PET scanning. PET scans were acquired in list mode over 15 minutes, 90 minutes after intravenous injection of a mean dose of 230 MBq of ^{18}F-AV-1451. The scans were iteratively reconstructed using a 3D-OSEM algorithm of four iterations and 12 subsets. Finally, they were smoothed with a Gaussian filter of 5mm full-width at half-maximum on a 128 x 128 matrix.

MRI scanning was performed using a 3T MAGNETOM Trio with a custom-built BrainPET insert in the bore of the magnet (Siemens, Erlangen, Germany). Vacuum cushions were used to reduce head motion.

T1-weighted images (MPRAGE) were acquired with the following parameters: repetition time (TR) 2250 ms; echo time (TE) 3.03 ms; flip angle 9°; 176 sagittal slices; resolution 1.0 x 1.0 x 1.0 mm^3). FMRI scans were acquired using an EPI sequence with the following parameters: TR = 2400 ms, TE = 30 ms, field of view = 210 mm, 36 slices, matrix size = 64 x 64, in-plane resolution = 3.3 x 3.3 mm^2, slice thickness 3 mm, distance factor = 10%, flip angle = 90°.

During the encoding session, 250 images were acquired. The field of view was angulated parallel to the medial cerebellar tentorium, to reduce susceptibility artifacts in the medial temporal lobe [43,44].

Processing of MRI data

Each participant's T1-image was segmented and parcellated using *FreeSurfer* (Version 6, https://surfer.nmr.mgh.harvard.edu; [45–47] . Following this process, cortical thickness, hippocampal volume, and total intracranial volume were derived. Hippocampal volume was divided by the total intracranial volume to account for differences in head size in subsequent analyses. The first eleven images of the encoding fMRI time series, during which instructions were presented to the participants, were discarded from analysis to ensure that the MR signal had reached a steady state.

Consequently, 239 images entered the analysis. fMRI data analysis was performed with FSL (FMRIB's Software Library, Version 5.0, http://www.fmrib.ox.ac.uk/fsl), employing different modules of the FSL-software package, specified as follows: Non-brain tissue was removed using BET [48]. Each time series's EPI images were spatially realigned with MCFLIRT [49] to correct for head movements between scans. Resulting fMRI time-series were spatially smoothed using a Gaussian kernel with FWHM = 8 mm, and a high-pass temporal filter (125 s) was applied. Based on the realignment parameters, participants with excessive head motion (maximum relative displacement of > 3mm) were excluded from further analysis. In the remaining data sets, FSLMotionOutliers was used to compute DVARS (D stands for the temporal derivative of timecourses, and VARS refers to root mean squared (RMS) variance over voxels; [50]), a measure of head motion based on the rate of change in the BOLD (blood oxygen level-dependent) signal across the whole brain at each timepoint.

Furthermore, FSLMotionOutliers was used to identify timepoints corrupted by head motion and enter them in a confound matrix included in the general linear model (GLM) to censor these timepoints. In addition to this confound matrix, global signal, white matter signal, the signal of the large arteries at the base of the brain, CSF signal, and the six motion parameters were included as covariates of no interest. GLM time-series statistical analysis of individual data sets was carried out using FILM (FMRIB's Improved Linear Model) with local autocorrelation correction [51].

Trials during the encoding phase can be divided into three types of events: trials where items presented during encoding were later correctly identified as "old" (OC), trials where items presented during encoding were later falsely identified as "new" (OF), and invalid trials (INV; i.e., misses and outliers). We primarily investigated neural activation during successful encoding, i.e., the OC trials. Additionally, neural activation underlying encoding can also be operationalized as the fMRI signal that is greater for stimuli that were later remembered than that for those later forgotten: the subsequent memory effect (SME). OC trials were contrasted against OF trials to analyze the SME.

A constant epoch regressor consisting of a boxcar function beginning at stimulus onset and lasting 3.5 s (stimulus duration) was defined for each event type. Additionally, for each event type, a variable epoch regressor with the identical timecourse as the respective constant epoch regressor, but variable boxcar width defined by the respective trial's response time was constructed. The variable epoch regressor was orthogonalized to the constant epoch regressor to account for the effects of response time variability, significantly influencing the amplitude of the hemodynamic response [52,53]. The resulting six regressors were convolved with a double gamma hemodynamic response function and entered into a first-level GLM analysis, together with the covariates listed above. Resulting statistical maps were transformed into the

space of the T1-image. For voxel-wise analyses, the statistical maps were normalized to standard space using nonlinear deformations obtained using the CAT12 toolbox (Computational AnatomyToolbox 12, http://www.neuro.uni-jena.de/cat/) implemented in SPM12 (www.fil.ion.ucl.ac.uk/spm/software/spm12). Second-level analyses of the fMRI data were performed using non-parametric testing as implemented in the FSL module *randomize* [54,55]. The non-parametric approach was chosen because of its statistical robustness in small sample sizes. Mean framewise displacement was included as a covariate of no interest. Framewise displacement was not correlated with any of the activation values used in the ROI analyses. Voxel-wise second-level analyses were constrained to gray matter. Threshold-free cluster enhancement [56] and family-wise error (FWE)-correction were employed to correct for multiple testing. Voxels with $p < 0.05$ are reported as significant.

For correlation analyses, parameter estimates (betas) for the constant epoch regressors of OC trials (remembered items) and OF trials (forgotten items) were extracted from the ROI described below.

PET processing

The PET images were processed as follows: (1) coregistration to the corresponding T1-image, (2) normalization to the lower cerebellar gray matter, (3) identification of unspecific binding sites, (4) partial volume correction using the Rousset approach. This resulted in partial volume corrected SUVR values for each cortical and subcortical region of interest (ROI) that were entered in the subsequent statistical analyses. The processing pipeline is described in detail in Baker et al., 2017 [57].

ROI analyses

The *FreeSurfer* ROI used in the partial volume correction of the AV1451 data served as the basis for the ROI analyses. Based on previous functional imaging studies of memory-related neural activation in cognitively healthy subjects [10,12,26,58], patients with Alzheimer's disease [29,59], and patients with Alzheimer's disease under cholinergic stimulation [27,28], the hippocampus, fusiform gyrus, and the PCC were selected as regions of interest.

The volume-weighted mean of the partial volume corrected SUVR of the cortical ROI corresponding to Braak stages I through VI [60] was computed as a global measure of cortical tau accumulation.

Results

Demographics and behavioral performance

Demographic and neuropsychological data for the sample that entered the imaging data analyses are presented in **Table 1**. Performance on the item memory task, quantified as d', was 1.208 ± 0.713 (minimum = 0.057, maximum = 2.692) and correlated with the delayed recall composite ($r_{(15)}$ = .636, 95%-CI [.154, .913]), but not the memory loss composite ($r_{(15)}$ = -.363, 95%-CI [-.755, .127]).

fMRI: Whole-brain activation

Neural activation during encoding of subsequently remembered items was observed in an extended network encompassing the fusiform gyrus, the lateral occipital cortex, temporoparietal areas, and primary sensory and motor cortices (**Fig. 1, Table 2**). During trials with subsequently remembered items, deactivation was observed in a pattern overlapping with the so-called "default mode network", including posterior midline structures, the anterior cingulate, lateral occipital cortices, as well as lateral temporal areas (**Fig. 1, Table 3**). An SME was not observed at the whole brain or ROI level.

Whole-brain AV1451-uptake

Tau accumulation, i.e., AV1451 uptake divided by the uptake in cerebellar gray matter, was most pronounced in the lateral temporal and the parietal lobe, with less retention in the frontal lobes (**Fig. 2**). This pattern is consistent with the histopathological staging, according to Braak and colleagues [61] and has been reported in several PET studies of Alzheimer's disease [60,62–64].

ROI analyses

Entorhinal tau accumulation was positively correlated with hippocampal activation for remembered items ($r_{(15)}$ = .670, p = .006, 95%-CI [.429, .826]; **Fig. 4A**). This correlation remained significant when correcting for delay between PET and MRI measurements ($r_{(12)}$ = .670, 95%-CI [.264, .880]), and medication ($r_{(12)}$ = .644, 95%-CI [.246, .856]), and after accounting for multiple comparisons. Entorhinal tau accumulation was not correlated with hippocampal activation for subsequently forgotten items (**Fig. 4A and B**).

Tau protein accumulation was not significantly associated with local neural activation in the PCC or the fusiform gyrus.

To determine if the association between entorhinal tau depositions and hippocampal neural activation was specific to these tau depositions, we correlated neural activation for subsequently remembered items with tau depositions averaged across the six Braak stages. Hippocampal activation for subsequently remembered items was not correlated with global tau accumulation. Furthermore, hippocampal volume and entorhinal cortex thickness were not significantly associated with hippocampal activation for subsequently remembered items.

Neural activation, tau accumulation, and cognition in the medial temporal lobe

To further elucidate the possible consequences of the association between entorhinal tau accumulation and neural activation, we examined how local activation and tau accumulation were related to memory function measures.

The memory loss composite score was positively correlated with entorhinal tau accumulation ($r_{(15)}$ = .718, 95%-CI [.432, .901]) (**Fig. 4C**). This correlation was significant after accounting for the delay between MR and PET measurements,

medication, and multiple comparisons. The memory loss composite score also correlated positively with hippocampal activation ($r_{(15)}$ = .478, 95%-CI [.079, .783]), but missed significance when accounting for medication ($r_{(12)}$ = .442, 95%-CI [-.101, .788]).

The delayed recall composite correlated negatively with entorhinal tau accumulation ($r_{(15)}$ = -.489, 95%-CI [-.761, -.122]) (**Fig. 4D**). This correlation was not significant when accounting for the delay between PET and MRI measurements ($r_{(12)}$ = -.394, 95%-CI [.024, -.736]) or medication ($r_{(12)}$ = -.502, 95%-CI [.125, -.821]).

The delayed recall composite was not correlated with hippocampal activation. d' was not correlated with entorhinal tau accumulation or hippocampal activation.

Discussion

We demonstrate that entorhinal tau deposition is associated with greater hippocampal activation during the encoding of information in Alzheimer's disease patients at the stage of MCI and mild dementia. Furthermore, we observed that the amount of entorhinal tau accumulation and, to a lesser degree, hippocampal activation are positively correlated with memory loss over time. These associations were specific to the medial temporal lobe structures; neural activation in the fusiform gyrus and the PCC was not significantly associated with local or global tau accumulation.

Tau accumulation and neural activation

Entorhinal tau accumulation correlated positively with hippocampal activation for subsequently remembered items. While this has not previously been investigated using tau PET and fMRI in a patient sample, similar findings have been reported in normal cognitive aging [10,12,13]. Maass et al. observed greater neural activation in

the anterior temporal lobe and the hippocampus in tau-positive than tau-negative cognitively healthy participants. Marks and colleagues described a correlation between tau accumulation in Braak I/II areas and hippocampal activation for items subsequently misidentified, while Huijbers et al. observed hippocampal "encoding success activity" to be correlated with inferior temporal tau accumulation. In analogy to Huijbers and colleagues, we found hippocampal activation for subsequently remembered items associated with entorhinal tau accumulation. A possible explanation for tau accumulation association with different activation patterns is that Marks et al. used a pattern separation-completion paradigm.

In contrast, Huijbers and colleagues used a face memory encoding task, more similar to our visual item memory task. The most parsimonious explanation for the discrepancy regarding tau accumulation location associated with hippocampal activation between our study and Huijbers et al. are differences in the disease stage and tau burden, which were substantially greater in our sample. Huijbers and colleagues did not observe an association between tau accumulation in the entorhinal cortex and hippocampal activation and specially selected the inferior temporal cortex ROI as a proxy for the spread of tau accumulation to the neocortex since entorhinal tau accumulation is commonly observed in advanced age [64]. In our sample, however, entorhinal tau accumulation was much higher than in the samples reported by Huijbers and Johnson [12,64].

In cognitively healthy seniors, hippocampal hyperactivity has been linked to tau accumulation, while amyloid and APOE status appear to play a smaller role [12]. Amyloid status has been discussed to explain the equivocal findings regarding changes in hippocampal activation in MCI [23]. While all patients in our sample were amyloid positive, we cannot directly link amyloid load to hippocampal activation, since we lack a standard quantitative amyloid measure that allows comparisons across all

participants. However, based on the cascade of the pathology in Alzheimer's disease and its association with neurodegeneration and cognition [2,65–67], tau accumulation is more likely to drive hippocampal activation at the stage of MCI or mild dementia than amyloid.

Hippocampal activation and cognition: Aberrant hippocampal activation?

Hippocampal activation was not associated with performance on the item memory task, quantified with the measure *d'*. Huijbers and colleagues also did not find a correlation between *d'* and any imaging measure. This lack of correlation may result from the fact that performance in visual item memory and face encoding tasks is not solely dependent on medial temporal function, but also requires visual processing, reflected in the strong activation in higher-order visual areas such as the fusiform gyrus [12,26]. In late MCI and mild dementia, these areas are often also affected by hypometabolism, tau deposition (cf. **Fig. 2**), and atrophy, but not as severely and consistently as the medial temporal lobe [63,68,69]. To obtain a true measure of memory (dys-) function and account for confounding effects of content type and stimulus processing, we computed a memory loss composite from verbal and visual memory scores.

This memory loss composite correlated highly with entorhinal tau accumulation and weakly with hippocampal activation. In other words, entorhinal tau, and, to a lesser degree, hippocampal activation during encoding, are associated with imperfect memory, but tau accumulation better explains memory deficits than hippocampal activation. Hippocampal activation may still be contributing to more deficient memory formation since it was positively correlated with the amount of information that was forgotten, i.e., worse memory.

Since hippocampal activation associated with encoding success was correlated with entorhinal tau accumulation, this activation could have been interpreted as compensatory. However, this is unlikely as compensatory activation is expected to be related to improved performance [70] and not worse memory, as in our case. Furthermore, evidence from animal models, individuals at risk of developing Alzheimer's disease, and individuals at preclinical stages indicates a pathological role of increased hippocampal activation rather than a compensatory mechanism [71,72]. Hippocampal hyperactivity may also be the consequence of disinhibition resulting from a disconnection from cortical inputs [73]. Ultimately, an experimental intervention would be required to determine if the causal effects of neuronal activation on cognition are compensatory or detrimental. There are reports that amelioration of task-related hippocampal hyperactivation by low doses of the antiepileptic drug levetiracetam can improve memory performance in MCI [17,18]. However, patients in those studies were recruited based on clinical criteria. Therefore, it is unknown how the observed hyperactivation was related to Alzheimer's pathology or if Alzheimer's pathology was even present in all participants.

In summary, while we could demonstrate that entorhinal tau accumulation is positively correlated with hippocampal activation, further studies combining biomarkers of Alzheimer pathology and an experimental intervention will be necessary to determine the nature of tau-linked hippocampal activation.

Limitations

The study is limited by its relatively small sample size, a general problem in clinical populations [74,75]. However, we observed strong associations, arguably because we investigated a patient cohort, where disease burden is expected to be much greater than in cognitively healthy samples [10,12,13]. The strength of the observed

associations is all the more striking considering the delay between fMRI and PET measurements (207.47 days, standard deviation 191.71 days), which was a little higher, but still in the same order of magnitude as in studies investigating cognitively normal subjects [10,12]. Nonetheless, our key findings, the positive correlations between entorhinal tau accumulation, hippocampal activation, and memory loss over time, remained significant when accounting for the delay between measurements and psychoactive medication in a subset of patients. However, when interpretating these findings, it has to be taken into account that they may still have influenced the results despite the statistical correction for these factors.

To reduce the complexity of the fMRI task, a two-choice task was used. However, this is also a limitation, because control stimuli with scrambled images would have allowed for differentiation between the visual effect of stimulus presentation and stimulus encoding. This needs to be considered when interpreting the activation pattern, especially for visual areas.

Arguably, this study is also limited by the absence of a control group. However, it was performed this way, because we specifically sought to investigate in patients the association between tau accumulation and fMRI activation, which has consistently been reported in cognitively normal samples. Since the same fMRI task has been used to compare MCI patients to an age-matched control group [27], no additional insights were expected from the inclusion of a control group. In light of this, it was ethically problematic to perform AV1451-PET in a cognitively normal sample.

A further limitation is that a subset of patients (4 out of 15) had a formal dementia diagnosis. Given that early dementia and MCI are adjacent diagnoses along the continuum of Alzheimer's disease, and the fact that this subset did not differ significantly from the remaining patients in demographics and overall cognition, it is highly unlikely that fundamentally different pathophysiological mechanisms drove the

observed effects. Finally, this study is also limited by its cross-sectional design. Any inference regarding causality, therefore, needs to be regarded with caution.

Conclusions

The present *in vivo* data demonstrate that tau accumulation in the entorhinal cortex is associated with neural activation in the hippocampus. Especially entorhinal tau accumulation is negatively correlated with memory performance in symptomatic Alzheimer's disease, extending previous findings in cognitively healthy aging [10,12,13]. Our data provide evidence that the positive correlation between hippocampal activation and entorhinal tau accumulation is also present in the early symptomatic stages of Alzheimer's disease. However, hippocampal activation measured using fMRI does not appear as the primary determinant of memory function. The association between local tau accumulation and neural activation was specific to the medial temporal lobe, indicating that tau accumulation does not generally increase or attenuate neural activation locally at this disease stage. Thus, the present findings contribute to our pathophysiological understanding of the relationship between tau accumulation, neural activation, and memory in Alzheimer's disease at the stage of MCI and mild dementia and may help inform future longitudinal and interventional studies.

Funding: This work was supported by a grant from the Medical Faculty of the University of Cologne (Forschungspool Klinische Studien, #2620000301) and the Marga and Walter Boll Foundation (# 210-08-13), Kerpen, Germany, to GRF, JK, and OAO.

Conflict of Interest: The authors have no conflict of interest to report.

References

[1] Aisen PS, Cummings J, Jack CR, Morris JC, Sperling R, Frölich L, Jones RW, Dowsett SA, Matthews BR, Raskin J, Scheltens P, Dubois B (2017) On the path to 2025: understanding the Alzheimer's disease continuum. *Alzheimers Res Ther* **9**, 60.

[2] Jack CR, Bennett DA, Blennow K, Carrillo MC, Dunn B, Haeberlein SB, Holtzman DM, Jagust W, Jessen F, Karlawish J, Liu E, Molinuevo JL, Montine T, Phelps C, Rankin KP, Rowe CC, Scheltens P, Siemers E, Snyder HM, Sperling R, Contributors (2018) NIA-AA Research Framework: Toward a biological definition of Alzheimer's disease. *Alzheimers Dement* **14**, 535–562.

[3] Reiman EM, Quiroz YT, Fleisher AS, Chen K, Velez-Pardo C, Jimenez-Del-Rio M, Fagan AM, Shah AR, Alvarez S, Arbelaez A, Giraldo M, Acosta-Baena N, Sperling RA, Dickerson B, Stern CE, Tirado V, Munoz C, Reiman RA, Huentelman MJ, Alexander GE, Langbaum JB, Kosik KS, Tariot PN, Lopera F (2012) Brain imaging and fluid biomarker analysis in young adults at genetic risk for autosomal dominant Alzheimer's disease in the presenilin 1 E280A kindred: a case-control study. *Lancet Neurol* **11**, 1048–1056.

[4] Quiroz YT, Schultz AP, Chen K, Protas HD, Brickhouse M, Fleisher AS, Langbaum JB, Thiyyagura P, Fagan AM, Shah AR, Muniz M, Arboleda-Velasquez JF, Munoz C, Garcia G, Acosta-Baena N, Giraldo M, Tirado V, Ramírez DL, Tariot PN, Dickerson BC, Sperling RA, Lopera F, Reiman EM (2015) Brain Imaging and Blood Biomarker Abnormalities in Children With Autosomal Dominant Alzheimer Disease: A Cross-Sectional Study. *JAMA Neurol* **72**, 912–919.

[5] Bookheimer SY, Strojwas MH, Cohen MS, Saunders AM, Pericak-Vance MA, Mazziotta JC, Small GW (2000) Patterns of brain activation in people at risk for Alzheimer's disease. *N Engl J Med* **343**, 450–456.

[6] Johnson SC, Schmitz TW, Trivedi MA, Ries ML, Torgerson BM, Carlsson CM, Asthana S, Hermann BP, Sager MA (2006) The influence of Alzheimer disease family history and apolipoprotein E epsilon4 on mesial temporal lobe activation. *J Neurosci* **26**, 6069–6076.

[7] Kennedy KM, Rodrigue KM, Devous MD, Hebrank AC, Bischof GN, Park DC (2012) Effects of beta-amyloid accumulation on neural function during encoding across the adult lifespan. *Neuroimage* **62**, 1–8.

[8] Rieck JR, Rodrigue KM, Kennedy KM, Devous MD, Park DC (2015) The effect of beta-amyloid on face processing in young and old adults: A multivariate analysis of the BOLD signal. *Hum Brain Mapp* **36**, 2514–2526.

[9] Elman JA, Oh H, Madison CM, Baker SL, Vogel JW, Marks SM, Crowley S, O'Neil JP, Jagust WJ (2014) Neural compensation in older people with brain amyloid-β deposition. *Nat Neurosci* **17**, 1316–1318.

[10] Marks SM, Lockhart SN, Baker SL, Jagust WJ (2017) Tau and β-Amyloid Are Associated with Medial Temporal Lobe Structure, Function, and Memory Encoding in Normal Aging. *J Neurosci* **37**, 3192–3201.

[11] Sperling R, Mormino E, Johnson K (2014) The evolution of preclinical Alzheimer's disease: implications for prevention trials. *Neuron* **84**, 608–622.

[12] Huijbers W, Schultz AP, Papp K V, LaPoint MR, Hanseeuw B, Chhatwal JP, Hedden T, Johnson KA, Sperling RA (2019) Tau Accumulation in Clinically Normal Older Adults Is Associated with Hippocampal Hyperactivity. *J Neurosci* **39**, 548–556.

[13] Maass A, Berron D, Harrison TM, Adams JN, La Joie R, Baker S, Mellinger T, Bell RK, Swinnerton K, Inglis B, Rabinovici GD, Düzel E, Jagust WJ (2019) Alzheimer's pathology targets distinct memory networks in the ageing brain. *Brain* **142**, 2492–2509.

[14] Celone KA, Calhoun VD, Dickerson BC, Atri A, Chua EF, Miller SL, DePeau K, Rentz DM, Selkoe DJ, Blacker D, Albert MS, Sperling RA (2006) Alterations in memory networks in mild cognitive impairment and Alzheimer's disease: an independent component analysis. *J Neurosci* **26**, 10222–10231.

[15] Kircher TT, Weis S, Freymann K, Erb M, Jessen F, Grodd W, Heun R, Leube DT (2007) Hippocampal activation in patients with mild cognitive impairment is necessary for successful memory encoding. *J Neurol Neurosurg Psychiatry* **78**, 812–818.

[16] Trivedi MA, Murphy CM, Goetz C, Shah RC, Gabrieli JD, Whitfield-Gabrieli S, Turner DA, Stebbins GT (2008) fMRI activation changes during successful episodic memory encoding and recognition in amnestic mild cognitive impairment relative to cognitively healthy older adults. *Dement Geriatr Cogn Disord* **26**, 123–137.

[17] Bakker A, Albert MS, Krauss G, Speck CL, Gallagher M (2015) Response of the medial temporal lobe network in amnestic mild cognitive impairment to therapeutic intervention assessed by fMRI and memory task performance. *Neuroimage Clin* **7**, 688–698.

[18] Bakker A, Krauss GL, Albert MS, Speck CL, Jones LR, Stark CE, Yassa MA, Bassett SS, Shelton AL, Gallagher M (2012) Reduction of hippocampal hyperactivity improves cognition in amnestic mild cognitive impairment. *Neuron* **74**, 467–474.

[19] Petrella JR, Wang L, Krishnan S, Slavin MJ, Prince SE, Tran TT, Doraiswamy PM (2007) Cortical deactivation in mild cognitive impairment: high-field-strength functional MR imaging. *Radiology* **245**, 224–235.

[20] Small SA, Perera GM, DeLaPaz R, Mayeux R, Stern Y (1999) Differential regional dysfunction of the hippocampal formation among elderly with memory decline and Alzheimer's disease. *Ann Neurol* **45**, 466–472.

[21] Machulda MM, Ward HA, Borowski B, Gunter JL, Cha RH, O'Brien PC, Petersen RC, Boeve BF, Knopman D, Tang-Wai DF, Ivnik RJ, Smith GE, Tangalos EG, Jack CR (2003) Comparison of memory fMRI response among normal, MCI, and Alzheimer's patients. *Neurology* **61**, 500–506.

[22] Nellessen N, Rottschy C, Eickhoff SB, Ketteler ST, Kuhn H, Shah NJ, Schulz JB, Reske M, Reetz K (2015) Specific and disease stage-dependent episodic memory-related brain activation patterns in Alzheimer's disease: a coordinate-based meta-analysis. *Brain Struct Funct* **220**, 1555–1571.

[23] Huijbers W, Mormino EC, Schultz AP, Wigman S, Ward AM, Larvie M, Amariglio RE, Marshall GA, Rentz DM, Johnson KA, Sperling RA (2015) Amyloid-β deposition in mild cognitive impairment is associated with increased hippocampal activity, atrophy and clinical progression. *Brain* **138**, 1023–1035.

[24] Wu JW, Hussaini SA, Bastille IM, Rodriguez GA, Mrejeru A, Rilett K, Sanders DW, Cook C, Fu H, Boonen RA, Herman M, Nahmani E, Emrani S, Figueroa YH, Diamond MI, Clelland CL, Wray S, Duff KE (2016) Neuronal activity enhances tau propagation and tau pathology in vivo. *Nat Neurosci* **19**, 1085–1092.

[25] Krüger L, Mandelkow EM (2016) Tau neurotoxicity and rescue in animal models of human Tauopathies. *Curr Opin Neurobiol* **36**, 52–58.

[26] Kim H (2011) Neural activity that predicts subsequent memory and forgetting: a meta-analysis of 74 fMRI studies. *Neuroimage* **54**, 2446–2461.

[27] Richter N, Beckers N, Onur OA, Dietlein M, Tittgemeyer M, Kracht L, Neumaier B, Fink GR, Kukolja J (2018) Effect of cholinergic treatment depends on cholinergic integrity in early Alzheimer's disease. *Brain*.

[28] Rombouts SA, Barkhof F, Van Meel CS, Scheltens P (2002) Alterations in brain activation during cholinergic enhancement with rivastigmine in Alzheimer's disease. *J Neurol Neurosurg Psychiatry* **73**, 665–671.

[29] Golby A, Silverberg G, Race E, Gabrieli S, O'Shea J, Knierim K, Stebbins G, Gabrieli J (2005) Memory encoding in Alzheimer's disease: an fMRI study of explicit and implicit memory. *Brain* **128**, 773–787.

[30] Albert MS, DeKosky ST, Dickson D, Dubois B, Feldman HH, Fox NC, Gamst A, Holtzman DM, Jagust WJ, Petersen RC, Snyder PJ, Carrillo MC, Thies B, Phelps CH (2011) The diagnosis of mild cognitive impairment due to Alzheimer's disease: recommendations from the National Institute on Aging-Alzheimer's Association workgroups on diagnostic guidelines for Alzheimer's disease. *Alzheimers Dement* **7**, 270–279.

[31] McKhann GM, Knopman DS, Chertkow H, Hyman BT, Jack CR, Kawas CH, Klunk WE, Koroshetz WJ, Manly JJ, Mayeux R, Mohs RC, Morris JC, Rossor MN, Scheltens P, Carrillo MC, Thies B, Weintraub S, Phelps CH (2011) The diagnosis of dementia due to Alzheimer's disease: recommendations from the National Institute on Aging-Alzheimer's Association workgroups on diagnostic guidelines for Alzheimer's disease. *Alzheimers Dement* **7**, 263–269.

[32] Scheltens P, Leys D, Barkhof F, Huglo D, Weinstein HC, Vermersch P, Kuiper M, Steinling M, Wolters EC, Valk J (1992) Atrophy of medial temporal lobes on MRI in "probable" Alzheimer's disease and normal ageing: diagnostic value and neuropsychological correlates. *J Neurol Neurosurg Psychiatry* **55**, 967–972.

[33] Minoshima S, Frey KA, Koeppe RA, Foster NL, Kuhl DE (1995) A diagnostic approach in Alzheimer's disease using three-dimensional stereotactic surface projections of fluorine-18-FDG PET. *J Nucl Med* **36**, 1238–1248.

[34] Duits FH, Teunissen CE, Bouwman FH, Visser PJ, Mattsson N, Zetterberg H, Blennow K, Hansson O, Minthon L, Andreasen N, Marcusson J, Wallin A, Rikkert MO, Tsolaki M, Parnetti L, Herukka SK, Hampel H, De Leon MJ, Schröder J, Aarsland D, Blankenstein MA, Scheltens P, van der Flier WM (2014) The cerebrospinal fluid "Alzheimer profile": easily said, but what does it mean? *Alzheimers Dement* **10**, 713-723.e2.

[35] Knopman DS, Petersen RC (2014) Mild cognitive impairment and mild dementia: a clinical perspective. *Mayo Clin Proc* **89**, 1452–1459.

[36] Tombaugh TN, McIntyre NJ (1992) The mini-mental state examination: a comprehensive review. *J Am Geriatr Soc* **40**, 922–935.

[37] Stanislaw H, Todorov N (1999) Calculation of signal detection theory measures. *Behav Res Methods Instrum Comput* **31**, 137–149.

[38] Helmstaedter C, Lendt M, Lux S (2001) Verbaler Lern- und Merkfähigkeitstest.

[39] Chang YL, Bondi MW, Fennema-Notestine C, McEvoy LK, Hagler DJ, Jacobson MW, Dale AM, Initiative ADN (2010) Brain substrates of learning and retention in mild cognitive impairment diagnosis and progression to Alzheimer's disease. *Neuropsychologia* **48**, 1237–1247.

[40] Ptok M, Buller N, Kuske S, Hecker H (2005) [Verbal learning and memory test in children. Analysis of it environmental validity]. *HNO* **53**, 369–375.

[41] Rey A (1964) L'examen clinique en psychologie.

[42] Hochberg Y, Benjamini Y (1990) More powerful procedures for multiple significance testing. *Stat Med* **9**, 811–818.

[43] Deichmann R, Gottfried JA, Hutton C, Turner R (2003) Optimized EPI for fMRI studies of the orbitofrontal cortex. *Neuroimage* **19**, 430–441.

[44] Weiskopf N, Hutton C, Josephs O, Deichmann R (2006) Optimal EPI parameters for reduction of susceptibility-induced BOLD sensitivity losses: a whole-brain analysis at 3 T and 1.5 T. *Neuroimage* **33**, 493–504.

[45] Dale AM, Fischl B, Sereno MI (1999) Cortical surface-based analysis. I. Segmentation and surface reconstruction. *Neuroimage* **9**, 179–194.

[46] Fischl B, Salat DH, Busa E, Albert M, Dieterich M, Haselgrove C, van der Kouwe A, Killiany R, Kennedy D, Klaveness S, Montillo A, Makris N, Rosen B, Dale AM (2002) Whole brain segmentation: automated labeling of neuroanatomical structures in the human brain. *Neuron* **33**, 341–355.

[47] Fischl B, Salat DH, van der Kouwe AJ, Makris N, Ségonne F, Quinn BT, Dale AM (2004) Sequence-independent segmentation of magnetic resonance images. *Neuroimage* **23 Suppl 1**, S69-84.

[48] Smith SM (2002) Fast robust automated brain extraction. *Hum Brain Mapp* **17**, 143–155.

[49] Jenkinson M, Bannister P, Brady M, Smith S (2002) Improved optimization for the robust and accurate linear registration and motion correction of brain images. *Neuroimage* **17**, 825–841.

[50] Power JD, Barnes KA, Snyder AZ, Schlaggar BL, Petersen SE (2012) Spurious but systematic

correlations in functional connectivity MRI networks arise from subject motion. *Neuroimage* **59**, 2142–2154.

[51] Woolrich MW, Ripley BD, Brady M, Smith SM (2001) Temporal autocorrelation in univariate linear modeling of FMRI data. *Neuroimage* **14**, 1370–1386.

[52] Richter N, Warbrick T, Mobascher A, Brinkmeyer J, Musso F, Stoecker T, Shah NJ, Fink GR, Winterer G (2013) Epoch versus impulse models in the analysis of parametric fMRI studies. *Clin Neurophysiol* **124**, 956–966.

[53] Grinband J, Wager TD, Lindquist M, Ferrera VP, Hirsch J (2008) Detection of time-varying signals in event-related fMRI designs. *Neuroimage* **43**, 509–520.

[54] Nichols TE, Holmes AP (2002) Nonparametric permutation tests for functional neuroimaging: a primer with examples. *Hum Brain Mapp* **15**, 1–25.

[55] Winkler AM, Ridgway GR, Webster MA, Smith SM, Nichols TE (2014) Permutation inference for the general linear model. *Neuroimage* **92**, 381–397.

[56] Smith SM, Nichols TE (2009) Threshold-free cluster enhancement: addressing problems of smoothing, threshold dependence and localisation in cluster inference. *Neuroimage* **44**, 83–98.

[57] Baker SL, Maass A, Jagust WJ (2017) Considerations and code for partial volume correcting [18F]-AV-1451 tau PET data. *Data Br.* **15**, 648–657.

[58] Garoff RJ, Slotnick SD, Schacter DL (2005) The neural origins of specific and general memory: the role of the fusiform cortex. *Neuropsychologia* **43**, 847–859.

[59] Huijbers W, Vannini P, Sperling RA, C M P, Cabeza R, Daselaar SM (2012) Explaining the encoding/retrieval flip: memory-related deactivations and activations in the posteromedial cortex. *Neuropsychologia* **50**, 3764–3774.

[60] Schöll M, Lockhart SN, Schonhaut DR, O'Neil JP, Janabi M, Ossenkoppele R, Baker SL, Vogel JW, Faria J, Schwimmer HD, Rabinovici GD, Jagust WJ (2016) PET Imaging of Tau Deposition in the Aging Human Brain. *Neuron* **89**, 971–982.

[61] Braak H, Alafuzoff I, Arzberger T, Kretzschmar H, Del Tredici K (2006) Staging of Alzheimer disease-associated neurofibrillary pathology using paraffin sections and immunocytochemistry. *Acta Neuropathol* **112**, 389–404.

[62] Ossenkoppele R, Schonhaut DR, Schöll M, Lockhart SN, Ayakta N, Baker SL, O'Neil JP, Janabi M, Lazaris A, Cantwell A, Vogel J, Santos M, Miller ZA, Bettcher BM, Vossel KA, Kramer JH, Gorno-Tempini ML, Miller BL, Jagust WJ, Rabinovici GD (2016) Tau PET patterns mirror clinical and neuroanatomical variability in Alzheimer's disease. *Brain* **139**, 1551–1567.

[63] Dronse J, Fliessbach K, Bischof GN, von Reutern B, Faber J, Hammes J, Kuhnert G, Neumaier B, Onur OA, Kukolja J, van Eimeren T, Jessen F, Fink GR, Klockgether T, Drzezga A (2017) In vivo Patterns of Tau Pathology, Amyloid-β Burden, and Neuronal Dysfunction in Clinical Variants of Alzheimer's Disease. *J Alzheimers Dis* **55**, 465–471.

[64] Johnson KA, Schultz A, Betensky RA, Becker JA, Sepulcre J, Rentz D, Mormino E, Chhatwal J, Amariglio R, Papp K, Marshall G, Albers M, Mauro S, Pepin L, Alverio J, Judge K, Philiossaint M, Shoup T, Yokell D, Dickerson B, Gomez-Isla T, Hyman B, Vasdev N, Sperling R (2016) Tau positron emission tomographic imaging in aging and early Alzheimer disease. *Ann Neurol* **79**, 110–119.

[65] Arriagada P V, Growdon JH, Hedley-Whyte ET, Hyman BT (1992) Neurofibrillary tangles but not senile plaques parallel duration and severity of Alzheimer's disease. *Neurology* **42**, 631–639.

[66] Nelson PT, Alafuzoff I, Bigio EH, Bouras C, Braak H, Cairns NJ, Castellani RJ, Crain BJ, Davies P, Del Tredici K, Duyckaerts C, Frosch MP, Haroutunian V, Hof PR, Hulette CM, Hyman BT, Iwatsubo T, Jellinger KA, Jicha GA, Kövari E, Kukull WA, Leverenz JB, Love S, Mackenzie IR, Mann DM, Masliah E, McKee AC, Montine TJ, Morris JC, Schneider JA, Sonnen JA, Thal DR, Trojanowski JQ, Troncoso JC, Wisniewski T, Woltjer RL, Beach TG (2012) Correlation of Alzheimer disease neuropathologic changes with cognitive status: a review of the literature. *J Neuropathol Exp Neurol* **71**, 362–381.

[67] Bischof GN, Jessen F, Fliessbach K, Dronse J, Hammes J, Neumaier B, Onur O, Fink GR, Kukolja J, Drzezga A, van Eimeren T, Initiative ADN (2016) Impact of tau and amyloid burden on glucose metabolism in Alzheimer's disease. *Ann Clin Transl Neurol* **3**, 934–939.

[68] Bejanin A, Schonhaut DR, La Joie R, Kramer JH, Baker SL, Sosa N, Ayakta N, Cantwell A, Janabi M, Lauriola M, O'Neil JP, Gorno-Tempini ML, Miller ZA, Rosen HJ, Miller BL, Jagust WJ, Rabinovici GD (2017) Tau pathology and neurodegeneration contribute to cognitive impairment in Alzheimer's disease. *Brain* **140**, 3286–3300.

[69] Teipel S, Drzezga A, Grothe MJ, Barthel H, Chételat G, Schuff N, Skudlarski P, Cavedo E, Frisoni GB, Hoffmann W, Thyrian JR, Fox C, Minoshima S, Sabri O, Fellgiebel A (2015) Multimodal imaging in Alzheimer's disease: validity and usefulness for early detection. *Lancet Neurol* **14**, 1037–1053.

[70] Cabeza R, Albert M, Belleville S, Craik FIM, Duarte A, Grady CL, Lindenberger U, Nyberg L, Park DC, Reuter-Lorenz PA, Rugg MD, Steffener J, Rajah MN (2018) Maintenance, reserve and compensation: the cognitive neuroscience of healthy ageing. *Nat Rev Neurosci* **19**, 701–710.

[71] Haberman RP, Branch A, Gallagher M (2017) Targeting Neural Hyperactivity as a Treatment to Stem Progression of Late-Onset Alzheimer's Disease. *Neurotherapeutics* **14**, 662–676.

[72] Palop JJ, Mucke L (2016) Network abnormalities and interneuron dysfunction in Alzheimer disease. *Nat Rev Neurosci* **17**, 777–792.

[73] Tahmasian M, Pasquini L, Scherr M, Meng C, Förster S, Mulej Bratec S, Shi K, Yakushev I, Schwaiger M, Grimmer T, Diehl-Schmid J, Riedl V, Sorg C, Drzezga A (2015) The lower hippocampus global connectivity, the higher its local metabolism in Alzheimer disease. *Neurology* **84**, 1956–1963.

[74] Conwell K, von Reutern B, Richter N, Kukolja J, Fink GR, Onur OA (2018) Test-retest variability of resting-state networks in healthy aging and prodromal Alzheimer's disease. *Neuroimage Clin* **19**, 948–962.

[75] Pardoe HR, Kucharsky Hiess R, Kuzniecky R (2016) Motion and morphometry in clinical and nonclinical populations. *Neuroimage* **135**, 177–185.

Tables

Table 1. Summary demographics and neuropsychological performance.

Demographic Data		
	Mean (SD)	N
Age	69.86 (7.03)	15
Gender (m/f)		10 ♂ / 5 ♀
Education [years]	15.93 (3.54)	15
Disease duration [years]	3.64 (1.42)	15
Neuropsychological Data		
MMST	25.47 (2.95)	15
GDS	2.97 (3.64)	15
Verbal memory$_{DR}$	2.93 (2.34)	15
Verbal memory$_{Loss}$	2.6 (2.59)	15
Visual memory$_{DR}$	5.47 (4.99)	15
Visual memory$_{Loss}$	26 (7.79)	15
TMT-A	67.81 (43.02)	15
TMT-B	176.71 (74.35)	15
Visual item memory fMRI task		
Items remembered [%]	61 (14)	15
Items forgotten [%]	30 (13)	15
Missed responses [%]	9 (3)	15
New stimuli classified as new [%]	73 (14)	15
New stimuli classified as old [%]	26 (14)	15
d'	1.21 (0.71)	15
Biomarkers		
CSF Aß 1-42	669.31 (171.39)	10
CSF total tau	524 (198.67)	10
CSF phospho tau	104.9 (52.22)	10
CSF tau / Aß 1-42 ratio	1.01 (0.51)	10
Amyloid-PET		10
Tau-PET		15
Days between Tau PET and MRI	207.47 (191.71)	15

MMSE = Mini-Mental-Status Exam; GDS = Geriatric Depression Scale; Verbal memory$_{DR}$ = delayed recall of the Verbal Learning Memory Test; Verbal memory$_{Loss}$ = immediate recall – delayed recall of the Verbal Learning Memory Test; ROCF$_{Loss}$ =

immediate recall - delayed recall of the Rey Osterrieth Complex Figure Test; $ROCF_{DR}$ = delayed recall of the Rey Osterrieth Complex Figure Test; TMT = Trail Making Test. CSF = cerebrospinal fluid. Either Amyloid-PET or CSF data were available from each participant. Standard deviations are presented in parentheses.

Table 2. Local maxima for the group average of activations associated with subsequently remembered items.

Structure	Side	x	y	z	T-value
Postcentral gyrus	left	-52	-22	50	15.8
Temporal occipital fusiform cortex	left	-30	-46	-20	12.6
Cerebellum, anterior lobe	left	-32	-44	-28	10.9
Precentral gyrus	left	-40	-16	54	9.81
Lateral occipital cortex, inferior division	left	-44	-70	-2	9.69
Temporal occipital fusiform cortex	right	38	-60	-16	15.5
Inferior temporal gyrus, temporooccipital part	right	50	-56	-16	12.1
Lateral occipital cortex, inferior division	right	40	-82	-4	11.8
Supplementary motor cortex	right	8	6	60	8.63
Precentral gyrus	right	42	6	22	7.46
Postcentral gyrus	right	38	-36	50	7.03
Inferior frontal gyrus, pars opercularis	right	46	12	26	6.95
Superior frontal gyrus	right	12	4	64	6.4
Superior parietal lobule	right	32	-56	52	6.32
Supramarginal gyrus, anterior division	right	58	-20	40	6.03
Lateral occipital cortex, superior division	right	32	-66	34	5.15

$p < 0.05$, FWE-corrected with cluster free threshold enhancement. Coordinates are reported in MNI-space.

Table 3. Local maxima for the group average of deactivations associated with subsequently remembered items.

Structure	Side	x	y	z	T-value
Precuneus	left	-2	-66	20	14
Cingulate gyrus, posterior division	left	-4	-52	32	10.8
Paracingulate gyrus	left	-6	40	26	9.66
Lateral occipital cortex, superior division	left	-52	-64	26	8.49
Angular gyrus	left	-58	-56	34	8.16
Middle temporal gyrus, anterior division	left	-54	2	-20	8.16
Superior frontal gyrus	left	-22	34	44	6.67
Frontal pole	left	-20	52	2	6.44
Lingual gyrus	left	-18	-62	-4	4.54
Angular gyrus	right	56	-46	30	10.3
Cingulate gyrus, anterior division	right	2	30	24	10.2
Middle frontal gyrus	right	26	26	40	8.88
Superior temporal gyrus, posterior division	right	60	-28	6	8.78
Planum temporale	right	50	-24	8	8.11
Temporal pole	right	58	10	-22	8.03
Central opercular cortex	right	40	-16	20	7.79
Lateral occipital cortex, superior division	right	56	-60	30	6.94
Superior frontal gyrus	right	24	28	52	6.78
Frontal pole	right	44	48	-4	4.53

$p < 0.05$, FWE-corrected with cluster free threshold enhancement. Coordinates are reported in MNI-space.

Figures

Figure 1

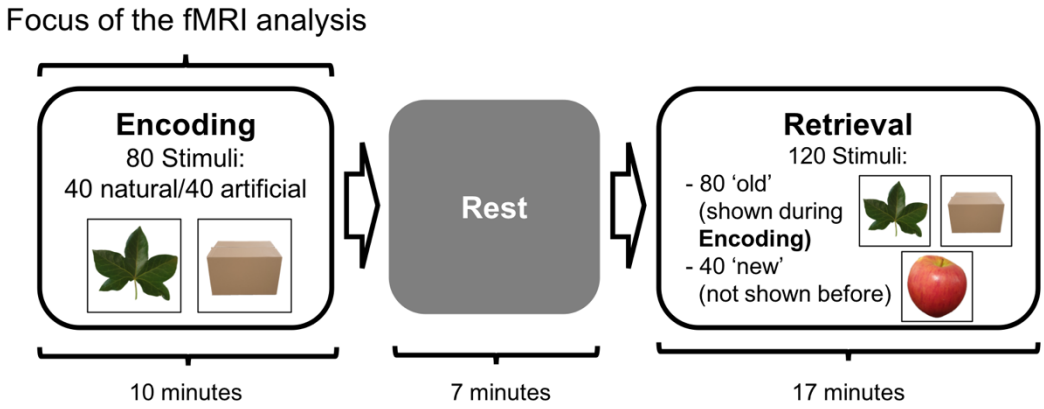

Schematic representation of the visual item memory task illustrating the order of task phases. The encoding and retrieval phases were separated by a 7-minute rest period. Also depicted are example visual stimuli. During encoding, participants were instructed to memorize stimuli and indicate whether the stimuli are natural or artificial via a button press. During retrieval, participants indicated via a button press if the stimuli were 'old' (presented during encoding) or 'new' (not previously presented).

Figure 2

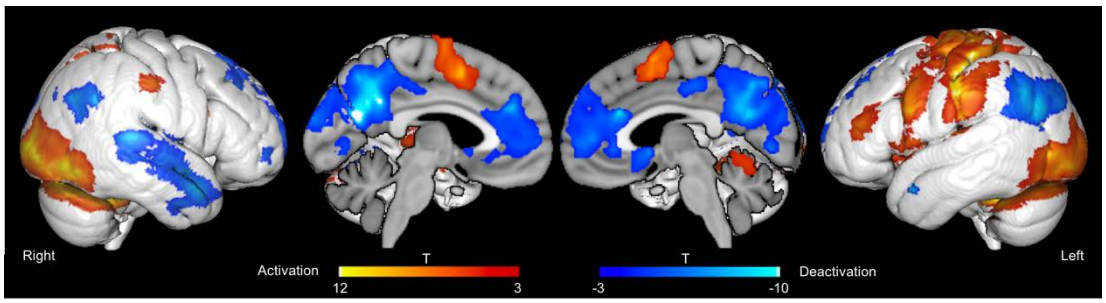

fMRI activation and deactivation for subsequently remembered stimuli. $p < 0.05$, FWE-corrected with cluster free threshold enhancement.

Figure 3

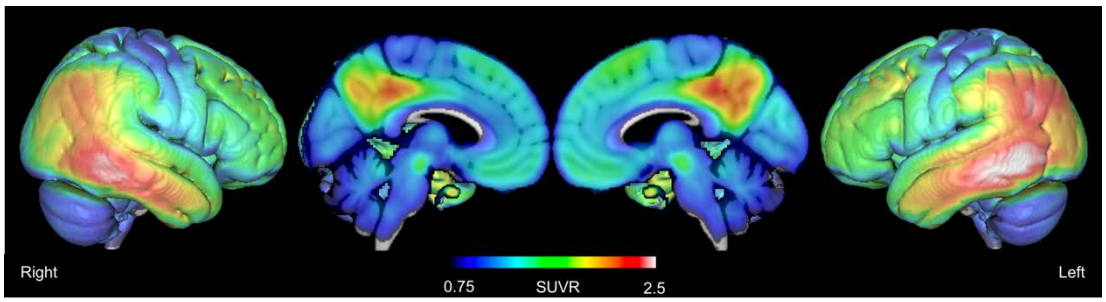

Average AV-1451 retention, normalized to cerebellar grey matter.

Figure 4

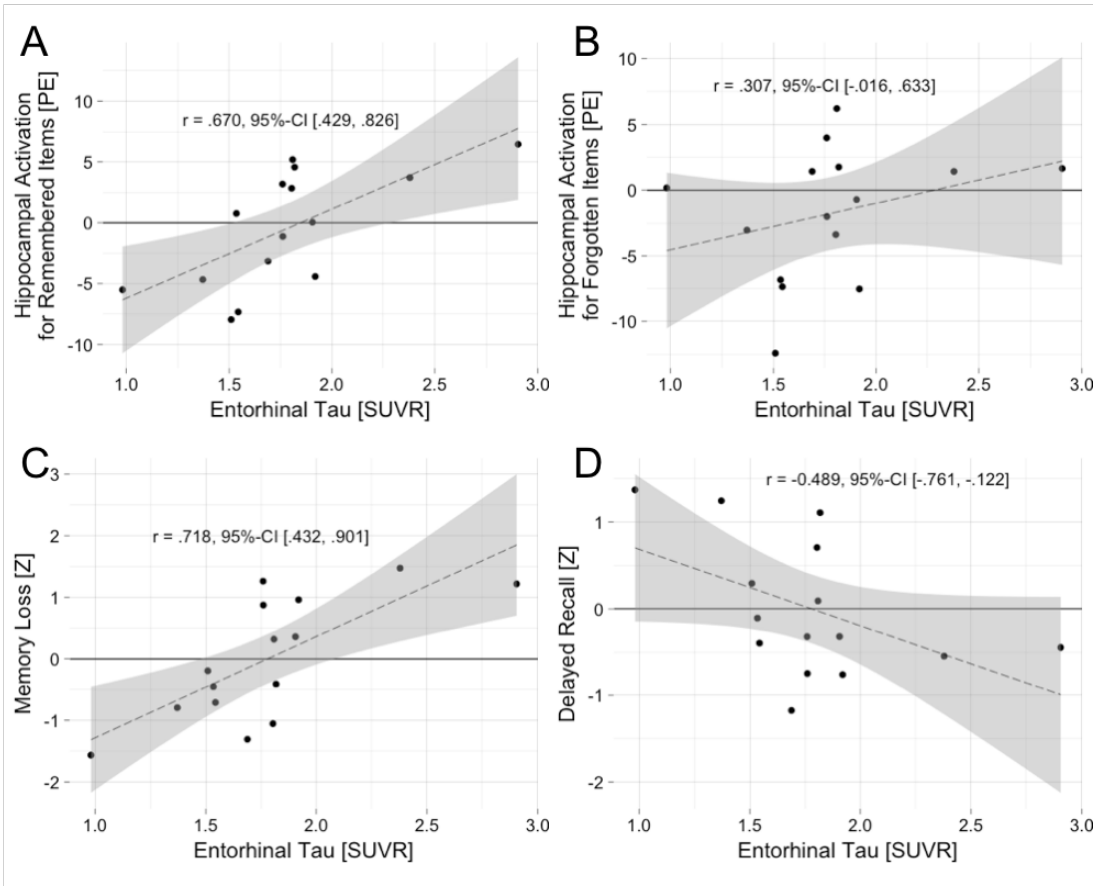

Entorhinal tau accumulation is associated with hippocampal activation and poorer memory performance. Entorhinal tau accumulation correlates with hippocampal activation during encoding of subsequently remembered items (A), but not with activation for subsequently forgotten items (B). Entorhinal tau accumulation also correlates with memory loss after a delay (C) and shows a trend towards a negative correlation with delayed recall performance (D). PE = parameter estimates. SUVR = standardized uptake value ratio.

Supplementary Table 1. Statistical values for correlations that did not meet statistical significance.

Measure 1	Measure 2	r	p-value (p-FDR < 0.0068)	95%-Confidence Interval	
				Lower	Upper
PCC tau accumulation	PCC activation for subsequently remembered items	-0.553	0.033	-0.808	-0.102
Fusiform gyrus tau accumulation	Fusiform gyrus activation for subsequently remembered items	-0.183	0.515	-0.634	0.516
Global tau accumulation	Hippocampal activation for subsequently remembered items	-0.313	0.256	-0.791	0.306
Hippocampal volume	Hippocampal activation for subsequently remembered items	-0.514	0.05	-0.857	0.098
Entorhinal cortex thickness	Hippocampal activation for subsequently remembered items	-0.272	0.327	-0.666	0.145
Delayed recall composite	Hippocampal activation for subsequently remembered items	-0.065	0.819	-0.497	0.531
d'	Hippocampal activation for subsequently remembered items	0.374	0.17	-0.315	0.822
d'	Entorhinal tau accumulation	-0.225	0.42	-0.672	0.387

FDR = false detection rate, PCC = posterior cingulate cortex